Generalized Langevin theory for gas/solid processes: Dynamical solid models

S. A. Adelman* and B. J. Garrison

Department of Chemistry, Purdue University, West Lafayette, Indiana 47907
(Received 16 June 1976)

A new class of smooth and structured solid models is developed from the generalized Langevin theory of gas/solid processes [S. A. Adelman and J. D. Doll, J. Chem. Phys. 64, 2375 (1976)], and numerical results for scattering off the simplest of these model solids are presented. The models, which may be refined to arbitrary precision, allow one to treat the many-body or lattice effect in gas/solid dynamics in a qualitatively correct but computationally simple manner. Scattering calculations based on the models may be carried out using standard classical trajectory methodology; the many-body dynamics modifies the usual classical equations of motion through noise terms and auxiliary variables. Collisional studies based on the simplest of the new models reveal the importance of many-body dynamics on energy transfer and trapping thresholds. The percentage of energy transfer due to many-body effects is found to be a rapidly increasing function of solid Debye temperature Θ_D; at $\Theta_D \gtrsim 225$°K the many-body contribution to energy transfer often exceeds the uncoupled oscillator contribution. The threshold energy for trapping on the simplest model solid is often more than doubled due to many-body influence. Finally, helium scattering from silver is simulated and the results are compared with the measurements of Sau and Merrill.

I. INTRODUCTION

Scattering, desorption, reaction, and other gas/solid processes are subtle and complex.[1] For the theorist, the challenge is to unravel microscopic mechanisms by developing and studying models detailed enough to mimic the essentials of real systems. Available models ignore a key feature, the many-body or coupled oscillator nature of the solid. Models which exclude many-body effects are qualitatively inadequate for desorption, diffusion, and other processes slow on the time scale of an atomic vibration. Residence times for trapped particles, for example, are roughly a Debye period for an Einstein (uncoupled oscillator) solid but may be much longer for real solids due to energy dissipation into the lattice. For scattering without trapping, a fast process, the importance of many-body effects is less obvious. The collision may be completed before the compressional wave created by the incident gas atom has time to propagate into the lattice, and an uncoupled oscillator model may suffice. The numerical calculations presented below (Sec. VI) show that even for nontrapping collisions, the many-body influence must be included in order to quantitatively describe gas/solid scattering attributes. The many-body contribution to energy transfer, for example, increases rapidly with surface Debye temperature Θ_D and often exceeds the uncoupled oscillator contribution for $\Theta_D \gtrsim 225$ °K (see Sec. VI).

We show here that the computational difficulties associated with the many-body problem (in classical mechanics) have now largely been overcome. We show, in particular, that a new class of computationally tractable solid models incorporating the many-body effect may be developed from the generalized Langevin theory of gas/solid processes.[2-5] The numerical labor involved in solving the simplest of our models is comparable to that involved in a three-particle classical trajectory calculation. Even the simplest model, however, describes the many-body effect in a qualitatively correct manner. The new models are suggested by the structure of the generalized Langevin equation (GLE). This is[4]

$$\ddot{x}(t) = -\omega_0^2 x(t) + \int_0^t \Theta(t-\tau)x(\tau)\,d\tau + R(t)\,, \tag{1.1a}$$

or equivalently

$$\ddot{x}(t) = -\Omega^2 x(t) - \int_0^t \beta(t-\tau)\,\dot{x}(\tau)\,d\tau + R_\beta(t), \tag{1.1b}$$

where

$$\Omega^2 = k_B T/\langle x^2\rangle,$$

$$\beta(t) = [k_B T]^{-1}\,\Phi(t) = \int_t^\infty \Theta(\tau)\,d\tau, \tag{1.2}$$

and

$$R_\beta(t) = R(t) - \beta(t)\,x(0). \tag{1.3}$$

The functions $\Theta(t)$ and $\beta(t)$ appearing in Eqs. (1.1) are response functions for the heat bath,[6] $x(t)$ is the coordinate of the struck solid atom, $R(t)$ is a Gaussian random force or thermal noise source, k_B is Boltzmann's constant, and T is the solid temperature. The fluctuation-dissipation theorem[4] links $R(t)$ and $\Theta(t)$ by

$$\langle \dot{R}(t)\dot{R}(0)\rangle = k_B T\,\Theta(t), \tag{1.4a}$$

or equivalently

$$\langle R(t)R(0)\rangle = k_B T\,\beta(t) = \Phi(t). \tag{1.4b}$$

The fluctuation-dissipation theorem expresses the balance between energy loss and gain processes, which enforces the decay of fluctuations from thermal equilibrium.

The average $\langle R(t)R(0)\rangle$ contains all relevant (i.e., statistical) information about the random force.[7] Thus Eqs. (1.1) and (1.4) show that the influence of the heat bath on the collision enters *solely* through $\Theta(t)$. This clean separation between lattice and collisional problems suggests a fruitful viewpoint basic to our models. Since the heat bath enters the theory only through its response characteristics, it may be replaced by an *equivalent* dynamical system with identical or nearly identical response characteristics. How "nearly identical" the characteristics of the equivalent system must be of course depends on the problem. For gas/solid processes, only the grosser features of the heat bath response are important. The response function of the equivalent system must adequately represent $\Theta(t)$ for short times and must decay for long times. The essential features are displayed by the response characteristics of a short chain of damped, noisy harmonic oscillators. Our models thus amount to replacing the heat bath by a damped harmonic chain (or chains) whose response characteristics optimally mimic those of the heat bath. Our simplest model for the heat bath is a single noisy damped harmonic oscillator. Our models are akin to an idea familiar in electronics, the method of equivalent circuits. The electrical analog of our simplest model is, in fact, the simplest high frequency LC filter. The electronics analogy will be made explicit below.

We develop the models as approximants to the exact response characteristics of the heat bath in Secs. II and III and Appendices A and B. In Sec. II and Appendix A we derive useful damped trigonometric expansions for $\Theta(t)$, Eqs. (2.8) and (2.11). A one term truncation yields our simplest model and collisional calculations (Sec. VI) show it to be remarkably satisfactory. Section III deals with an analogous representation for $R(t)$, Eq. (3.17). The key results of Secs. II and III are that the heat bath can be modeled by a few (~ 1) *damped* harmonic oscillators when computing $\Theta(t)$ and may be represented by *undamped* oscillators when computing $R(t)$. In Sec. IV we discuss anharmonic effects. We expect that the most important anharmonicity occurs in the self-force on the struck atom [the force which in the harmonic approximation is $-\omega_0^2 x(t)$] and is thus a one-body effect. When the self-force term is made anharmonic, the computed energy transfer typically decreases (Sec. VI). Many-body anharmonic corrections can also be made. We discuss this qualitatively in Sec. IV; elsewhere we will give a detailed treatment.[8]

In Sec. V we propose a class of smooth and structured dynamical solid models which will prove useful for computer simulations of scattering, desorption, diffusion, and reaction. Section VI describes our method for solving the GLE and gives numerical results for scattering of He, Ne, and Ar off the simplest of the model solids with the solid at both 0 °K and finite temperature. More extensive numerical work will shortly be presented elsewhere.[9]

Finally in Appendix C, we develop a least action principle for the classical GLE. This Lagrangian formulation provides a natural link between our classical theory and the Feynman[10] path integral form of quantum mechanics and hence connects our classical and semiclassical[5] Langevin approaches.

II. COMPACT REPRESENTATION FOR $\Theta(t)$

The kernel $\Theta(t)$ is developed in a form suitable for use in numerical solution of the GLE. We begin with the Laplace domain[11] relation betwen $\chi(t)$, the impulse response function of the struck oscillator, and $\Theta(t)$. It is[4]

$$\hat{\chi}^{-1}(z) = z^2 + \omega_0^2 - \hat{\Theta}(z). \tag{2.1}$$

Equation (2.1) is more usefully expressed in terms of the non-negative and even spectral density functions $\rho(\omega)$ and $\sigma(\omega)$ defined by

$$\chi(t) = \int_0^\infty \rho(\omega) \frac{\sin\omega t}{\omega}\, d\omega\,, \tag{2.2a}$$

$$\Theta(t) = \int_0^\infty \sigma(\omega) \frac{\sin\omega t}{\omega}\, d\omega\,. \tag{2.2b}$$

For harmonic solids $\rho(\omega)$ is the unit normalized mode density[12]; more generally it is a weighted density of transition frequencies of the solid.[8] The function $\sigma(\omega)$ is the analogous spectral density for the heat bath. [It is not unit normalized, however, since $\dot{\Theta}(0) \neq 1$.] Inversion of Eqs. (2.2) yields

$$\rho(\omega) = (-2\omega/\pi)\,\mathrm{Im}\,\hat{\chi}(i\omega)\,, \tag{2.3a}$$

$$\sigma(\omega) = (-2\omega/\pi)\,\mathrm{Im}\,\hat{\Theta}(i\omega)\,. \tag{2.3b}$$

Equations (2.3) are slightly disguised versions of the Kramers–Kronig relations as shown in Appendix B. From Eq. (2.1) one sees

$$\mathrm{Im}\,\hat{\Theta}(i\omega) = \mathrm{Im}\,\hat{\chi}(i\omega)/|\hat{\chi}(i\omega)|^2\,. \tag{2.4}$$

Comparison of Eqs. (2.3) and (2.4) therefore gives

$$\sigma(\omega) = \rho(\omega)/|\hat{\chi}(i\omega)|^2\,. \tag{2.5}$$

The relations (2.2a) and (2.5) show that the spectrum of the heat bath $\sigma(\omega)$ is easily computed from the more accessible[13] spectrum of the solid $\rho(\omega)$.

The ω dependence of the "screening factor" $|\chi(i\omega)|^2$ in Eq. (2.5) is interesting. For ω much less than the Debye or maximum frequency ω_D, $|\hat{\chi}(i\omega)|^2$ is nearly constant and thus $\sigma(\omega)$ is proportional to $\rho(\omega)$. For $\omega \lesssim \omega_D$, $|\hat{\chi}(i\omega)|^2$ typically becomes large [e.g., in the Debye model $\hat{\chi}(i\omega_D) = \infty$] due to near resonance with atomic bond frequencies and $\sigma(\omega)$ decreases. This behavior, which is illustrated in Fig. 1 for the Debye model, is plausible if we recall[4] that the heat bath is derived from the solid by clamping the struck oscillator at its equilibrium position. The local clamping quite reasonably distorts only the high frequency lattice vibrations.

Equations (2.2b) and (2.5) give the following useful representation for $\Theta(t)$:

$$\Theta(t) = \int_0^{\omega_D} \frac{\rho(\omega)}{|\hat{\chi}(i\omega)|^2} \frac{\sin\omega t}{\omega}\, d\omega\,, \tag{2.6}$$

where ω_D is the maximum frequency in the distribution $\rho(\omega)$. Converting Eq. (2.6) to an integral on the interval [0, 1] and evaluating by M-point quadrature yields

$$\Theta(t) \approx \omega_D^3 \sum_{\lambda=1}^{M} w_\lambda \frac{\sin\omega_\lambda t}{\omega_\lambda} \frac{\omega_D^{-3}\rho(\omega_\lambda)}{|\hat{\chi}(i\omega_\lambda)|^2}\,, \tag{2.7}$$

where w_λ and $x_\lambda = \omega_\lambda/\omega_D$ are quadrature weights and points. The expansion (2.7) is inefficient, since it attempts to synthesize an oscillatory decaying function $\Theta(t)$ by destructive interference. For times longer than $t' \gtrsim \pi M/\omega_0$, Eq. (2.7) breaks down and the approximate $\Theta(t)$ is undamped.

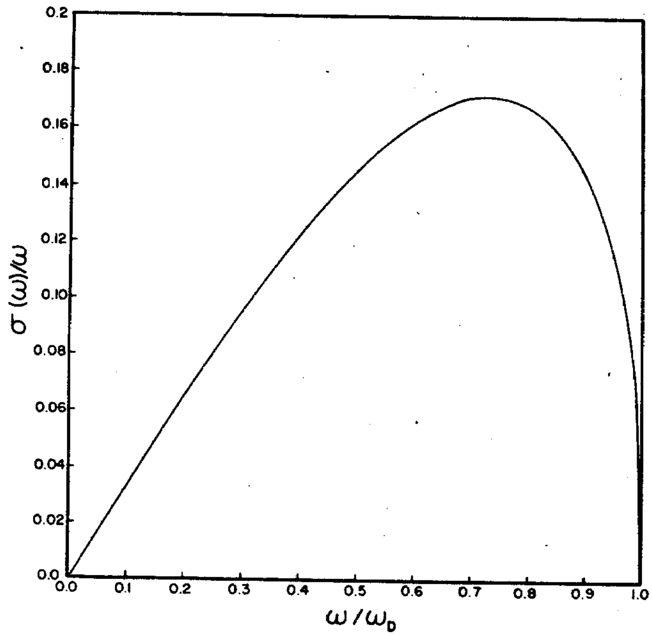

FIG. 1. Spectral density of the heat bath $[\sigma(\omega)/\omega]$ for the Debye model, $\rho(\omega) = [3/\omega_D^3]\omega^2\eta(\omega_D - \omega)$ as computed from Eq. (2.5). For $\omega \lesssim 0.3\omega_D$ the $\sigma(\omega)/\omega$ is linear; i.e., density is that of an acoustic continuum. Larger ω local damping distorts $\sigma(\omega)$.

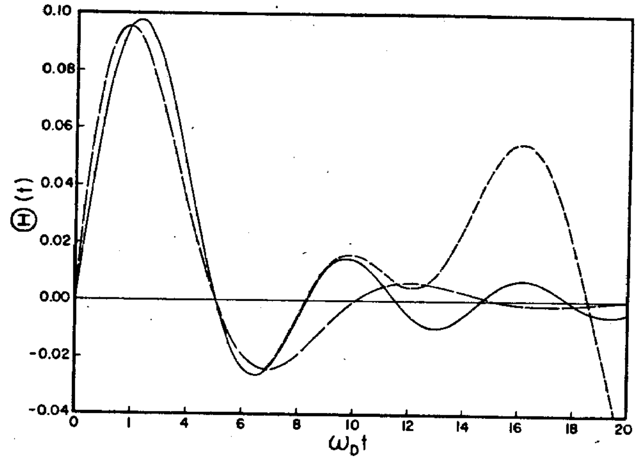

FIG. 3. Memory kernel $\Theta(t)$ for the Debye model vs $\omega_D t$. Exact Debye model results ——. One term damped oscillator approximant, Eq. (2.8), — —. Four term undamped oscillator approximant, Eq. (2.7), - - - - - -. The damped oscillator approximant is adequate in the important short-time regime and properly decays asymptotically; the four-term undamped oscillator approximant while excellent for short-times, is inadequate because of unphysical recurrences at longer times.

In physical terms, Eq. (2.7) amounts to modeling the heat bath by an effective linear chain of M *undamped* harmonic oscillators.[14] A compressional wave set up in this effective finite chain will be unphysically reflected by the chain boundaries rather than lost into the lattice. The first such reflection or recurrence will occur at $t \simeq t'$ and leads to the breakdown of (2.7) for $t \gtrsim t'$. Equation (2.7) is thus useless for computation of long duration gas/solid processes, since the spurious recurrences cause unphysically short residence times for trapped gas atoms.[15] Equation (2.7) is unsatisfactory even for direct scattering, since 6–12 quadrature points must be used and the computer time per trajectory increases roughly linearly with the number of quadrature points [Sec. VIA].

Rather than inefficiently modeling the heat bath by a long chain of undamped oscillators, one can efficiently model it by a short chain of damped oscillators. Such a representation eliminates recurrences. One procedure which works well is simply to expand

$$\Theta(t) = \sum_{\lambda=1}^{M} C_\lambda \sin\tilde{\omega}_\lambda t\, e^{-\gamma_\lambda t} \tag{2.8}$$

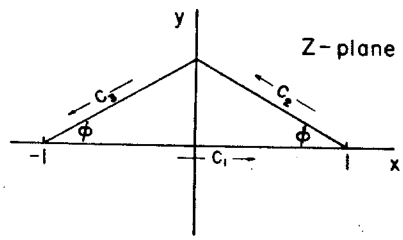

FIG. 2. Contour used in the transformation of Eq. (2.2) into Eq. (2.9).

and to fit C_λ, $\tilde{\omega}_\lambda$, and γ_λ by least squares to an accurate $\Theta(t)$ computed from a long expansion of the form (2.7).

An alternative scheme to approximate $\Theta(t)$ is based on the integral representation

$$\Theta(t) = \omega_D^3 \int_0^1 G(x)\, e^{-\gamma(x)\omega_D t}\, \frac{\sin[x\omega_D t - \delta(x)]}{x}\, dx \tag{2.9}$$

derived in Appendix A from Eq. (2.2b) via the contour in Fig. 2. In Eq. (2.9) $G(x)$, $\delta(x)$, and $\gamma(x)$ are the weight, phase, and damping functions defined in Eqs. (A5), (A6), and (A8). By Eq. (2.6), $\Theta(t=0) = 0$. Thus

$$\int_0^1 dx\, G(x)\, \frac{\sin\delta(x)}{x}\, dx = 0. \tag{2.10}$$

Combining Eqs. (2.9) and (2.10) and approximating the result by M-point quadrature gives

$$\Theta(t) = \omega_D^3 \sum_{\lambda=1}^{M} w_\lambda \frac{G(x_\lambda)}{x_\lambda}\, e^{-\gamma(x_\lambda)\omega_D t} \times \{\sin[x_\lambda \omega_D t - \delta(x_\lambda)] + \sin\delta(x_\lambda)\}\,. \tag{2.11}$$

Thus the contour method gives an expansion for $\Theta(t)$ in terms of *damped* oscillators with frequencies $\omega_\lambda = x_\lambda \omega_D$ and damping constants $\omega_D \gamma(x_\lambda)$. By including the $\sin\delta(x_\lambda)$ term in Eq. (2.11) we guarantee that the approximate $\Theta(t=0) = 0$.

In Fig. 3 we compare the exact Debye model $\Theta(t)$ with a *single* damped oscillator approximation [Eq. (2.8)] and a four term undamped oscillator approximation [Eq. (2.7)]. Inclusion of damping is clearly essential because of the incorrect long-time growth in the undamped case, and in fact the one-term damped oscillator approximant provides a representation of the Debye solid quite adequate for collisional studies (Sec. VI).

Thus, at least for the Debye solid, we have an important simplification, the systematic part of the influence of the heat bath on the collision is qualitatively that of a *single* damped harmonic oscillator.

III. SIMULATION OF $R(t)$

We now turn to an analogous development for $R(t)$, the unsystematic part of the influence of the heat bath on the collision. At least for harmonic solids $R(t)$ is a Gaussian random process.[4] Thus the probability $P[R(t)]$ for a particular $R(t)$ is

$$P[R(t)] \sim \exp\left[-\frac{1}{2}\int_{-\infty}^{\infty}\int_{-\infty}^{\infty} R(\tau)B(\tau-\tau')R(\tau')\,d\tau\,d\tau'\right], \tag{3.1}$$

where $B(t)$ is the inverse of $\Phi(t)=\langle R(t)R(0)\rangle$; i.e.,

$$\int_{-\infty}^{\infty} B(t-\tau)\Phi(\tau-t')\,d\tau=\delta(t-t') \ . \tag{3.2}$$

Equation (3.1) is simply the probability distribution function for a set of correlated Gaussian random variables $R(t_1)$, $R(t_2)$, ..., generalized to the continuous case.

We wish to sample $R(t)$ by Monte Carlo methods.[16] While one could select $R(t)$ from a discretized approximation to Eq. (3.1), this is inconvenient because (a) such an approximate Gaussian distribution is multidimensional [since $R(t)$ and $R(t')$, $t\neq t'$, are correlated], and because (b) we require $R(t)$ for continuous time intervals rather than at discrete times.

We avoid these difficulties by working with the Fourier domain form of Eq. (3.1),

$$P[R(t)] \sim \exp\left[\frac{-1}{4\pi}\int_{-\infty}^{\infty} d\omega\,\frac{|\tilde{R}(\omega)|^2}{\tilde{\Phi}(\omega)}\right], \tag{3.3}$$

where the two-sided Fourier transforms are

$$\tilde{R}(\omega)=\int_{-\infty}^{\infty} R(t)\,e^{i\omega t}\,dt \ , \tag{3.4}$$

$$\tilde{B}(\omega)=\int_{-\infty}^{\infty} B(t)\,e^{i\omega t}\,dt \ , \tag{3.5}$$

and

$$\tilde{\Phi}(\omega)=\tilde{B}^{-1}(\omega)=\int_{-\infty}^{\infty} e^{i\omega t}\,\Phi(t)\,dt \ . \tag{3.6}$$

Note that we have used Eq. (3.2) to obtain the first equality in Eq. (3.6). Further simplification follows from the symmetry properties

$$\tilde{R}(\omega)=\tilde{R}^*(-\omega) \tag{3.7}$$

and

$$\tilde{\Phi}(\omega)=\tilde{\Phi}(-\omega)=\Phi^*(\omega) \ , \tag{3.8}$$

which hold because $R(t)$ is real and $\Phi(t)$ is real and even. In the phase-amplitude representation,

$$\tilde{R}(\omega)=|\tilde{R}(\omega)|\,e^{i\delta(\omega)} \ , \tag{3.9}$$

Eq. (3.7) becomes

$$|\tilde{R}(\omega)|=|\tilde{R}(-\omega)| \ , \tag{3.10a}$$

with

$$\delta(\omega)=-\delta(-\omega) \ . \tag{3.10b}$$

Using Eqs. (3.9) and (3.10), the inverse of Eq. (3.4) becomes

$$R(t)=\frac{1}{\pi}\int_0^{\omega_D}|\tilde{R}(\omega)|\cos[\omega t - \delta(\omega)]\,d\omega \ . \tag{3.11}$$

Equation (3.3) similarly becomes

$$P[R(t)] \sim \exp\left[\frac{-1}{2\pi}\int_0^{\omega_D} d\omega\,\frac{|\tilde{R}(\omega)|^2}{\tilde{\Phi}(\omega)}\right]. \tag{3.12}$$

We have cut off the integrals in Eqs. (3.11) and (3.12) at the maximum frequency ω_D. This is permitted since (see below)

$$\tilde{\Phi}(\omega)=\pi k_B T\,\sigma(\omega)/\omega^2 \ , \tag{3.13}$$

and because $\sigma(\omega)$, by Eq. (2.5), is cut off at ω_D by $\rho(\omega)$.

We now establish Eq. (3.13). Using the evenness of $\Phi(t)$, one rewrites Eq. (3.6) as

$$\tilde{\Phi}(\omega)=2\mathrm{Re}\int_0^{\infty} e^{-i\omega t}\,\Phi(t)\,dt=2\,\mathrm{Re}\,\hat{\Phi}(i\omega) \ . \tag{3.14}$$

From Eq. (1.2)

$$\hat{\Phi}(z)=(k_B T/z)(\hat{\Theta}(0)-\hat{\Theta}(z)) \tag{3.15}$$

and thus

$$\tilde{\Phi}(\omega)=(-2k_B T/\omega)\,\mathrm{Im}\hat{\Theta}(i\omega) \ . \tag{3.16}$$

Equation (2.3b) with Eq. (3.16) gives Eq. (3.13).

Tractable approximations for $R(t)$ are developed by converting the integrals in Eqs. (3.11) and (3.12) to the interval [0, 1] and then evaluating by M-point quadrature. This yields

$$R(t)=\frac{\omega_D}{\pi}\sum_{\lambda=1}^{M} w_\lambda\,|\tilde{R}(\omega_\lambda)|\cos[\omega_\lambda t-\delta(\omega_\lambda)] \tag{3.17}$$

and

$$P[R(t)]=\prod_{\lambda=1}^{M} P_\lambda \ , \tag{3.18}$$

where

$$P_\lambda \sim \exp\left[\frac{-1}{k_B T}\,\frac{w_\lambda}{2\pi^2}\left(\frac{\omega_\lambda}{\omega_D}\right)^2\frac{|\tilde{R}(\omega_\lambda)|^2}{\omega_D^{-3}\,\sigma(\omega_\lambda)}\right]. \tag{3.19}$$

In Eqs. (3.17)–(3.19), w_λ and $x_\lambda=\omega_\lambda/\omega_D$ are quadrature weights and points (e.g., Gauss–Legendre) appropriate to the interval [0, 1].

The Fourier domain representation Eq. (3.12) is diagonal and consequently factors into products of univariate Gaussians. This is its advantage over the original time-domain representation. Monte Carlo sampling of $R(t)$ is thus easy. We select $|\tilde{R}(\omega_\lambda)|$ from P_λ, $\delta(\omega_\lambda)$ is selected from a uniform distribution with $0\le\delta(\omega_\lambda)\le 2\pi$, and $R(t)$ is constructed from Eq. (3.17).

Our procedure has a simple physical analog. It amounts to replacing the heat bath by an M-atom effective linear harmonic chain with normal modes ω_λ. These modes are coupled to the struck atom by the force constants

$$\Omega_\lambda^2 = \omega_D^2 [w_\lambda \omega_D^{-3} \sigma(\omega_\lambda)]^{1/2} \quad , \tag{3.20}$$

i.e.,

$$R(t) = \sum_{\lambda=1}^{M} \Omega_\lambda^2 \left[\xi_\lambda \cos\omega_\lambda t + \dot{\xi}_\lambda \frac{\sin\omega_\lambda t}{\omega_\lambda} \right]. \tag{3.21}$$

In Eq. (3.21) ξ_λ and $\dot{\xi}_\lambda$ are the initial positions and momenta of the normal modes of the effective chain given by

$$\xi_\lambda = \frac{1}{\pi}\left[\frac{w_\lambda}{\omega_D^{-3}\sigma(\omega_\lambda)}\right]^{1/2}\left(\frac{\omega_\lambda}{\omega_D}\right)\frac{|\tilde{R}(\omega_\lambda)|}{\omega_\lambda}\cos\delta(\omega_\lambda) \, , \tag{3.22}$$

$$\dot{\xi}_\lambda = \frac{1}{\pi}\left[\frac{w_\lambda}{\omega_D^{-3}\sigma(\omega_\lambda)}\right]^{1/2}\left(\frac{\omega_\lambda}{\omega_D}\right)|\tilde{R}(\omega_\lambda)|\sin\delta(\omega_\lambda) \, . \tag{3.23}$$

The initial conditions ξ_λ and $\dot{\xi}_\lambda$ are found from the initial phases $\delta(\omega_\lambda)$ and the initial energies

$$\begin{aligned} \epsilon_\lambda &= \tfrac{1}{2}[\dot{\xi}_\lambda^2 + \omega_\lambda^2 \xi_\lambda^2] \\ &= \frac{1}{2\pi^2}\,\frac{w_\lambda}{\omega_D^{-3}\sigma(\omega_\lambda)}\left(\frac{\omega_\lambda}{\omega_D}\right)^2 |\tilde{R}(\omega_\lambda)|^2 \end{aligned} \tag{3.24}$$

by the standard Monte Carlo procedure; i.e., the phases are chosen to be random and the energies are selected from the Boltzmann distribution

$$P_\lambda \sim e^{-\epsilon_\lambda/k_B T} \quad . \tag{3.25}$$

This effective chain correspondence is correct, since Eqs. (3.21) and (3.25) with (3.20) and (3.21)–(3.22) are identical to Eqs. (3.17)–(3.19).

IV. ANHARMONIC EFFECTS

Our development, so far, has been restricted to harmonic solids. The *linear* generalized Langevin structure is, however, fundamental[17] and tied in no way to the harmonic model. This suggests that the nonlinear GLE for scattering[4] may similarly be more general than its derivation. This is indeed true[8] if the reaction of the heat bath to the motion of the struck atom is treated within the linear response approximation[18] and if other less essential restrictions are satisfied. A detailed discussion will be presented elsewhere.[8] The key result is that *all* lattice dynamical information relevant to the scattering can be compressed into a free lattice response function and an associated noise source. Although the methodology for computing anharmonic responses is undeveloped, the associated correlation functions can be "measured" in molecular dynamics simulations.[19] Thus large-scale calculations may be needed to determine the anharmonic responses but once these are available gas/solid processes can be studied in small scale Langevin calculations. The contrast with a conventional trajectory study of scattering off a set of coupled oscillators is striking. There the lattice dynamics are, in effect, recomputed during each trajectory.

Our program here is much less ambitious than that outlined above. We only study the effects of anharmonicity in the binding potential of the struck atom. This is perhaps the dominant anharmonicity, since the struck atom is driven far up its potential wall during the collision. Neighboring atoms are disturbed less severely since the impact energy is distributed among ~4–8 neighbors.

Because the self-force anharmonicity is a one-body effect, it is trivially incorporated into the Langevin equation. One merely makes the substitution

$$\omega_0^2 x(t) \to -2\beta D_e e^{-\beta x(t)} [e^{-\beta x(t)} - 1] \tag{4.1}$$

in the Langevin equation. The Morse parameters β and D_e are determined from the binding energy of a surface atom[20] and from ω_0^2 which is the second moment of the frequency distribution, i.e.,

$$\omega_0^2 = \int_0^{\omega_D} \omega^2 \rho(\omega)\, d\omega. \tag{4.2}$$

This simple treatment of anharmonicity is clearly exact if the collision time τ_c is so short that many-body effects play no role; i.e., if the integral in Eq. (1.1) contributes negligibly for $t \le \tau_c$.

V. MODELS FOR GAS/SOLID PROCESSES

Our viewpoint here is that of linear systems theory.[21] The heat bath is regarded as a black box characterized solely by its causal response $\Theta(t)$. More detailed specification is irrelevant to the output; e.g., the collision cross section. Consequently the many-body heat bath may be modeled by fictitious few-body systems with similar response characteristics.

This idea has been exploited in other linear systems problems. A prototype is the modeling of a complex electrical network by a simple resistance R. Consider for example, the high frequency LC filter which is a near perfect analog of our solid. Figure 4 illustrates the analogy. An infinite harmonic chain coupled to a terminal cube is shown in Fig. 4(a). This is our effective chain, (i.e., Eq. (2.7) with $M=\infty$), which exactly mimics the influence of a spatially isotropic heat bath (for the anisotropic case the cube must be coupled to three nonparallel, nonidentical effective chains). The struck atom is drawn as a cube, since the simplest solid models ignore surface microstructure. The electrical analog of the chain, an LC transmission line, is shown in Fig. 4(b). Input signals of high frequency cannot penetrate far into the transmission line, so it acts as a *high frequency* filter. The chain displays analogous behavior in the time domain; compressional waves cannot penetrate far into the chain in *short times*. As shown in Fig. 4(d) the tail of the transmission line can be replaced by an equivalent impedance $Z(\omega)$ which duplicates its frequency response. The heat bath may similarly be replaced by an equivalent oscillator as in Fig. 4(c). Finally we may model $Z(\omega)$ by an effective resistance R with frequency independent response. This simplest LC filter is shown in Fig. 4(f). In the analogous solid model [Fig. 4(e)] the equivalent oscillator is modeled by a Brownian oscillator[22] with frequency $\tilde{\omega}_1$,

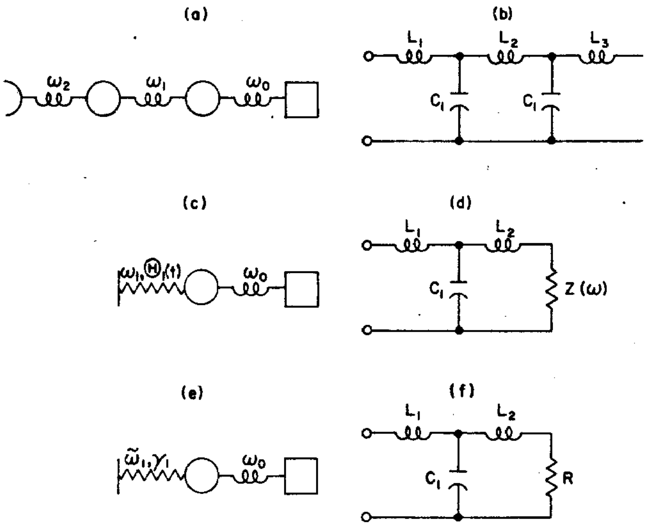

FIG. 4. Solid–circuit analogy. (a) The infinite effective harmonic chain. (b) The electrical analog an LC transmission line. (c) Rigorous replacement of the heat bath by a single harmonic oscillator with damping characteristics $\hat{\Theta}_1(z) = z^2 + \omega_1^2 - \hat{\Theta}^{-1}(z)$ [c.f., Eq. (2.1)]. (d) Analogous replacement of the tail of transmission line by an AC impedance $Z(\omega)$ with correct analytic structure. (e) Simplest solid model which generalizes the soft-cube model to include the many-body effect; the heat bath is approximated by a Brownian oscillator with a time-local friction constant γ_1 and frequency $\tilde{\omega}_1$. (f) Analogous circuit, the simplest LC filter; $Z(\omega)$ is approximated by a frequency independent resistance R.

and local damping constant γ_1. This amounts to truncating the sum in Eq. (2.8) at one term. The solid-circuit analogy holds for the noise as well as the damping. The impedances $Z(\omega)$ or R put out a random voltage (Johnson noise) whose autocorrelation is related to $Z(\omega)$ by a fluctuation-dissipation theorem (Nyquist Theorem).

Our simplest approximation for $\Theta(t)$, as illustrated in Fig. 4(e), provides a new model for studying gas/solid processes. It is a generalization of the soft-cube model[23] which includes many-body effects. Trajectory studies based on this new model are hardly more laborious than those based on an independent oscillator (Einstein) model. The results, however, are much more realistic since the many-body effect is accurately represented [Sec. VI].

The model of Fig. 4(e) may be extended to include surface microstructure. This is schematized in Fig. 5. Inclusion of surface structure is necessary in order to describe rainbow scattering,[24] diffraction,[25] diffusion and its competition with desorption, and probably reaction. We believe that the model of Fig. 5, augmented to include the anisotropy of lattice vibrations, contains those features of the solid which play an essential role in gas/solid dynamics. Because of its simplicity, the model will permit convenient computer simulation of many gas/solid processes.

The models just proposed are not the simplest imaginable. One may replace the struck oscillator itself by a Brownian oscillator and obtain a still simpler picture, a one-oscillator rather than a two-oscillator solid. Such a model is, however, inadequate, since it implies that the influence of the heat bath is instantaneously felt by the struck oscillator. Processes which are uninfluenced by the heat bath, i.e., processes which occur in a time $\tau \ll \omega_D^{-1}$, are consequently improperly treated within this single Brownian oscillator model for the solid. The simplest models which have *all* the correct qualitative features are those in which the *heat bath* rather than the full solid is replaced by a Brownian oscillator. These are, of course, the models proposed here.

VI. NUMERICAL METHODS AND RESULTS

A. Methods

Our problem is to numerically solve the GLE for scattering[4]

$$M\ddot{Y}(t) = -\partial W(x, Y)/\partial Y , \tag{6.1a}$$

$$\ddot{x}(t) = -\omega_0^2 x(t) + \int_0^t \Theta(t-\tau)\, x(\tau)\, d\tau + R(t) - \frac{\partial W(x, Y)}{\partial x} , \tag{6.1b}$$

where Y is the coordinate of the gas atom, x is the coordinate of the struck lattice atom, and $W(x, y)$ is the gas/solid interaction potential.

Our approximations for $\Theta(t)$ involve expansions in trigonometric, Eq. (2.7), or exponentially damped trigonometric, Eqs. (2.8) and (2.11), functions. These particular approximate basis functions allow $\Theta(t)$ to be expanded in a series of the form

$$\Theta(t-\tau) = \sum_{n=1}^{R} g_n(t)\, h_n(\tau) . \tag{6.2}$$

This sum of products form is important, since it means that the integral in Eq. (6.1b) need not be recomputed at each integration step.

Inserting Eq. (6.2) into (6.1b) and defining

$$H_n(t) = \int_0^t h_n(\tau) x(\tau)\, d\tau , \tag{6.3}$$

we can rewrite Eqs. (6.1) as the system of first-order equations

$$M\dot{Y}(t) = P(t) , \tag{6.4a}$$

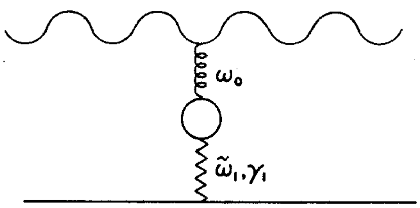

FIG. 5. Simple structured solid model which incorporates damping and noise [i.e., the many-body effect]. The wavy surface schematizes a periodic gas/solid potential. The heat bath is modeled by a single Brownian oscillator with $\tilde{\omega}_1$ and γ_1 chosen to give a best fit to $\Theta(t)$. By attaching additional (and in general different) effective chains to the surface, the model may be augmented to include lattice waves parallel as well as transverse to the surface plane (i.e., surface phonons.)

$$\dot{P}(t) = -\partial W(x, Y)/\partial Y, \tag{6.4b}$$

$$\dot{x}(t) = p(t), \tag{6.4c}$$

$$\dot{p}(t) = -\omega_0^2 x(t) + \sum_{n=1}^{R} g_n(t) H_n(t) - \frac{\partial W(x, Y)}{\partial x} + R(t), \tag{6.4d}$$

$$\dot{H}_n(t) = h_n(t) x(t). \tag{6.4e}$$

Equations (6.4) may be solved using integration methods[26] standard in classical trajectory work. The only new feature is that the contribution of the *external force* $R(t)$ must be included.

The importance of a compact representation for $\Theta(t)$ is now evident. The more terms in Eq. (6.2) the larger is the system Eq. (6.4). Fortunately a one-term or single *damped* oscillator representation of $\Theta(t)$ gives an excellent description of the many-body effect on the scattering for the cases studied. With this $\Theta(t)$ solving Eq. (6.4) is equivalent in labor to computing scattering off a two-atom chain. The full many-body effect is, however, obtained from the Langevin calculation because of the inclusion of damping in $\Theta(t)$. As we have stressed repeatedly, this damping is essential for processes lasting longer than, say, a Debye period. If damping is ignored, then unphysical reflections of energy back to the struck oscillator lead to a qualitatively incorrect description of the process.

One additional technical point must be dealt with. The noise $R(t)$ and the initial position of the struck oscillator are not statistically uncorrelated. This is because the noise involves the initial positions of the heat bath atoms, which are statistically correlated with $x(0)$. This correlation makes simultaneous Monte Carlo sampling of $x(0)$ and $R(t)$ awkward. We avoid the difficulty by setting $x(0) = 0$. This is always permissible, since the time at which the collision begins is arbitrary.[27] In essence, this allows the random force $R(t)$ to bring the position of the struck atom into a thermal distribution before the impinging gas atom reaches the interaction region.

B. Results and discussion

We have solved the generalized Langevin equations (6.4) for scattering of rare gas atoms from metals. We present representative results here, leaving the specifics of the calculations and the complete results to a future report.[9] In this study, we report results for Ne and Ar scattering from metals (Ne/metal) and (Ar/metal) with the solid temperature at 0 °K and He/Ag scattering at nonzero solid temperatures.

Before solving the generalized Langevin equations an approximate $\Theta(t)$ must be determined. When the solid temperature is 0 °K, classically there is no motion of the solid atoms, allowing only one trajectory as the solution to Eqs. (6.4). The random force [Eq. (3.17) and (3.16)] and the initial position and momentum of the struck atom are zero; therefore, no Monte Carlo averaging is needed. Thus the testing for an accurate representation for $\Theta(t)$ was done at a solid temperature of 0 °K. Approximating $\Theta(t)$ by a small number of quadrature points [Eq. (2.7)] was unsatisfactory, as it relied on destructive interference of oscillatory functions to produce decay at long times (Fig. 3). By least squares fitting $\Theta(t)$ at short times to a damped oscillatory function (Eq. 2.8) we guarantee long time decay. Table I displays the effect of varying the number of damped oscillatory functions in the approximation to $\Theta(t)$ on the energy transfer in Ar/metal scattering. Columns 3–5 give the energy transfer for 1, 2, and 3 functions in the approximate $\Theta(t)$ as a function of Debye temperature Θ_D. One damped sine term is within ~1%–2% of the three term approximant. This is a negligible difference when compared to energy transfer without many-body effects, i.e., $\Theta(t) = 0$ (column 2). Although the single damped sine function does not perfectly reproduce the exact $\Theta(t)$ at short times (Fig. 3), the effect of the error on the energy transfer is small (at least for these short duration collisions). A critical factor in representing $\Theta(t)$ is having $\Theta(t)$ decay at long times. Thus for our calculations we used one damped sine function to represent $\Theta(t)$.

TABLE I. Influence of approximate $\Theta(t)$ functions on Ar/metal energy transfer at three surface Debye temperatures Θ_D. Potential parameters are those for Ar/Ag scattering; kinetic energy of the beam is 2500 °K oriented at 45° from the surface normal, surface temperature = 0 °K. Columns 3–5 give results for 1–3 term damped oscillator approximants to Debye model $\Theta(t)$. Column 2 gives results when many-body effect [i.e., $\Theta(t)$] is set equal to zero.

		ΔE(°K)		
Θ_D(°K)	$\Theta(t)=0$	$M=1$	$M=2$	$M=3$
151	1145	1223	1220	1214
200	812	956	952	943
250	517	710	707	697

Notice that the many-body contribution to the energy transfers given in Table I is never larger than ~37%. This is not typical; rather it is due to the high Ar beam energy (2500 °K) employed in the calculations in Table I. Because of this high beam temperature (lower beam temperatures give trapping in Ar scattering), the collision time is short enough so that the single oscillator approximation [$\Theta(t)=0$] is not grossly inaccurate. For room temperature beams, many-body influence is much more important.

This influence is shown in Fig. 6 where we plot, as an example, energy transfer in Ne/metal scattering as a function of the surface Debye temperature Θ_D. The solid temperature is 0 °K and the gas–metal potential parameters used were those for the Ne/Ag interaction. Equations (6.4) were solved using both a harmonic and an anharmonic (Morse) self-potential [Eq. (4.1)] for the struck oscillator and with and without many-body effects. The difference in energy transfer between the many-body oscillator and the single oscillator increases with surface Debye temperature. At $\Theta_D \gtrsim 225$ °K the many-body effect is larger than the single oscillator energy transfer. The single oscillator curve has the right shape, but to get a quantitative result many-body effects must be included. Using an anharmonic Morse potential has only a small effect on the energy transfer.

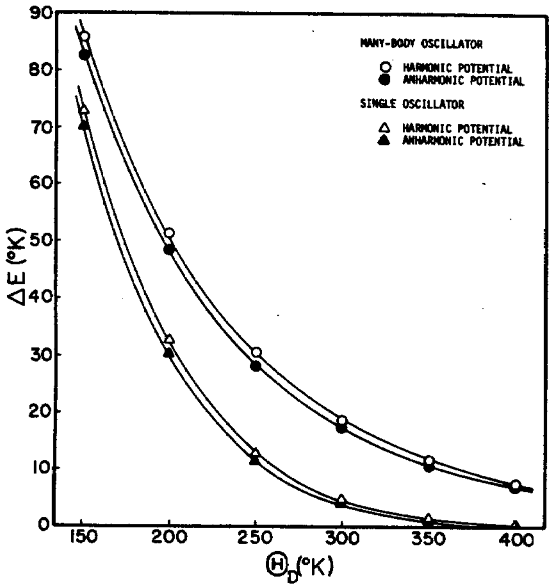

FIG. 6. Many-body and anharmonic effects on energy transfer ΔE in Ne/Ag scattering as a function of surface Debye temperature. The kinetic energy of the Ne is 296 °K oriented at 45° from the surface normal. The surface temperature is 0 °K.

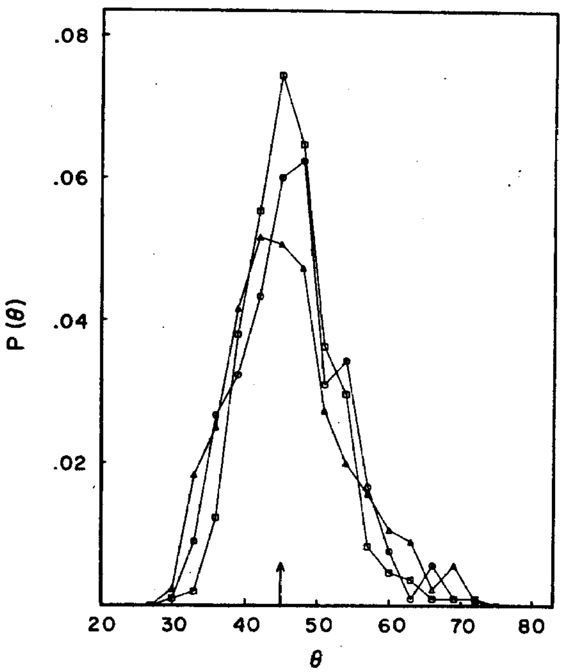

FIG. 7. Angular distributions of He/Ag scattering at solid temperatures of 296 °K (□), 373 °K (○), and 573 °K (△). The kinetic energy of the He is 296 °K oriented at 45° from the surface normal.

The Morse potential is more repulsive thus the energy transfer is less than that for the harmonic potential. Since the anharmonic effects are small in the struck atom, it is plausible that no serious mistakes are being made by assuming the rest of the solid to be harmonic (see Sec. IV).

For the Ar/metal system we found that the trapping threshold (maximum beam kinetic energy at which the Ar trapped on the surface) to be very sensitive to many-body effects and anharmonicity. (See Table II.) At a surface Debye temperature of 151 °K (appropriate to Ag) the trapping threshold for a harmonic potential including many-body effects is 2200 °K. If an anharmonic potential is used the threshold reduces to 1600 °K, 27% lower. The threshold is reduced even further if only a single oscillator approximation is used, 1250 °K for the harmonic potential and 900 °K for the anharmonic potential. At the higher surface Debye temperature of 250 °K, the energy transfer is much less and the differences in trapping thresholds are less drastic, but still large. Thus for a system like Ar/metal where energy transfer is large, both the many-body effects and the anharmonic potential should be included.

TABLE II. Trapping thresholds for Ar/metal scattering with the Ar oriented at 45° from the surface normal, $T=0$ °K, for single oscillator $[\Theta(t)=0]$ and many-body $[(\Theta(t)\neq 0]$ models of the solid.

	Trapping threshold (°K)	
Θ_D(°K)	$\Theta(t)=0$	$\Theta(t)\neq 0$
151	1250	2200
	900[a]	1600[a]
250	75	250
	50[a]	200[a]

[a]Anharmonic correction in self-force of struck atom included as discussed in Sec. IV and Ref. 9.

In solving the GLE for He/Ag we used nonzero solid temperatures so to compare with the experimental data of Sau and Merrill[28] and the theoretical calculations of Lin and Wolken.[29] The kinetic energy of the He atoms was 296 °K. The angle of incidence was 45° from the surface normal. The solid temperatures were 296, 373, and 573 °K. We arbitrarily chose to use four terms in Eq. (3.17) for the random force. Further testing must be done to ascertain that these results are converged. Angular distributions are shown in Fig. 7. As was seen in Sau and Merrill's data, He/Ag scattering is quasielastic, having the maximum of scattered intensity at the specular angle. In qualitative agreement with experiment, the intensity of the specular peak decreases with increasing solid temperature. Since we have neglected out-of-plane scattering, we cannot make a quantitative comparison of peak heights and widths. In a future study we plan to include surface phonons and thus be able to determine the out-of-plane scattering. Our results are also in qualitative agreement with the quantum calculations of Lin and Wolken.[29]

VII. SUMMARY AND DISCUSSION

A new class of solid models which properly include many-body dynamics are developed from the generalized Langevin equation (GLE). Numerical calculations of rare gas scattering off the simplest of these models, which replaces the heat bath by a single damped noisy harmonic oscillator, are presented. The models derive from the idea that only rather gross features of the heat bath's complex dynamics importantly influence gas/solid processes, and these gross features are displayed by a single (optimally chosen) damped harmonic oscillator. More precisely, the heat bath response function $\Theta(t)$ may be replaced by a much simpler model response function $\Theta_M(t)$. The response function $\Theta_M(t)$ must resemble $\Theta(t)$ at short times and decay at long times.

The great advantage of the models is that they yield a computationally simple theory which fully incorporates many-body dynamics. Solving the GLE for our simplest model is comparable in labor to solving a three-body classical trajectory problem.

Our numerical results demonstrate that many-body influence is important quantitatively in rare gas/metal scattering. Anharmonic effects, while not negligible, are typically smaller. We find specifically that the many-body effects contribute importantly to the energy transfer in Ne/silver scattering, but that the contribution due to the anharmonicity of the solid is small. However, for scattering of Ar, a more massive atom, the anharmonicity of the solid as well as the many-body effect dramatically influences the maximum energy at which the Ar is trapped on the solid. Angular distributions of He/Ag scattering are given for the solid temperatures of 296, 373, and 573 °K. The scattering is predominantly specular, in qualitative agreement with the experimental results of Sau and Merrill.

ACKNOWLEDGMENTS

We wish to acknowledge support of this work by a Research Corporation Cottrell Research grant. This work was partially supported by the National Science Foundation (MRL program DMR 76-00889). We also thank Professor J. D. Doll of SUNY, Stony Brook for continued valuable conversations and correspondence.

APPENDIX A

We now derive Eq. (2.9) from Eq. (2.2). We explicitly consider $\Theta(t)$, but our development is equally valid for $\chi(t)$. We first rewrite Eq. (2.2b) as

$$\Theta(t)=\frac{\omega_D^3}{2i}\int_{-1}^{1} g(x)\frac{e^{ix\tau}}{x}\,dx\ , \tag{A1}$$

where $x=\omega/\omega_D$, $\tau=\omega_D t$, and $g(x)=\omega_D^{-3}\,\sigma(\omega)$ is a dimensionless mode density. We have used $\sigma(\omega)=\sigma(-\omega)$ and $\sigma(0)=0$ to obtain Eq. (A1). We assume $g(z)$ is analytic inside the contour in Fig. (2), as discussed below, and rewrite Eq. (A1) as

$$\Theta(t)=(-1/2i)(I_2+I_3)\ , \tag{A2}$$

where

$$I_2=\int_{C_2} g(z)\,\frac{e^{iz\tau}}{z}\,dz\ , \tag{A3}$$

and where I_3 is the corresponding integral along C_3.

One may verify that $I_3=-I_2^*$.

Thus

$$\Theta(t)=-\operatorname{Im} I_2\ . \tag{A4}$$

Along C_2

$$z=x+i\tan\phi\,[1-x]\ ,\qquad dz=e^{-i\phi}\sec\phi\,dx\ . \tag{A5}$$

We will also require the phases $\beta(x)$ and $\eta(x)$ and the amplitudes $r(x)$ and $G(x)$ defined by

$$z=r(x)\,e^{i\beta(x)}\ , \tag{A6a}$$

$$g(z)=(r(x)\cos\phi/x)\,G(x)\,e^{-i\eta(x)}\ . \tag{A6b}$$

Using Eqs. (A5) and (A6) in Eq. (A3) then gives

$$I_2=-\int_0^1 dx\ e^{i[x+i\tan\phi(1-x)]\tau}\,\frac{G(x)}{x}\,e^{-i[\phi+\eta(x)+\beta(x)]}\ . \tag{A7}$$

Combining Eqs. (A4) and (A7) finally yields Eq. (2.9) with

$$\delta(x)=\phi+\eta(x)+\beta(x),\quad \gamma(x)=\tan\phi(1-x)\ . \tag{A8}$$

For the Debye model $\Theta(t)$, $\eta(x)=-2\beta(x)$ and $\delta(x)=\phi-\beta(x)$.

The angle ϕ is chosen to optimize the accuracy of the quadrature approximant, Eq. (2.11). We have found $35°\lesssim\phi\lesssim45°$ to be best.

We now return to the analyticity assumption. For the Debye model $\Theta(t)$, it is valid for $|z|<1$; i.e., for $\phi<45°$. For real solids it is not strictly valid because of van Hove singularities in the mode density. The problem disappears if we work with approximate analytic densities, for example densities found by Montroll's method.[13] Some error is incurred with approximate densities, since the singularities dominate the long-time behavior of the response functions.[12] For our purposes, the error is unimportant, since $\Theta(t)\to0$ at $t\to\infty$ and therefore the long-time part of $\Theta(t)$ contributes negligibly to the integral in Eq. (6.1b).

APPENDIX B

We show here that Eqs. (2.2) and (2.3) are equivalent to the Kramers–Kronig relations, e.g.,

$$\tilde{\chi}'(\omega)=\frac{P}{\pi}\int_{-\infty}^{\infty} d\omega'\,\frac{\tilde{\chi}''(\omega')}{\omega'-\omega}\ , \tag{B1}$$

linking the real and imaginary parts of the complex susceptibility

$$\tilde{\chi}(\omega)=\tilde{\chi}'(\omega)+i\,\tilde{\chi}''(\omega)=\int_0^{\infty} e^{i\omega t}\,\chi(t)\,dt\ . \tag{B2}$$

Our plan is to derive (B1) from Eqs. (2.2) and (2.3). We begin with

$$\chi''(\omega)=\int_0^{\infty}\sin\omega t\,\chi(t)\,dt$$

$$=-\operatorname{Im}\int_0^{\infty}\chi(t)\,e^{-i\omega t}\,dt=-\operatorname{Im}\hat{\chi}(i\omega)\ , \tag{B3}$$

which follows from Eq. (B2). Comparing Eqs. (2.3) and (B3) gives

$$\tilde{\chi}''(\omega)=(\pi/2\omega)\,\rho(\omega). \tag{B4}$$

The dissipative part of the susceptibility $\tilde{\chi}''(\omega)$ is odd by Eq. (B3) so $\rho(\omega)$ is even as asserted earlier.

Combining Eqs. (2.2), (B2), and (B4) gives

$$\tilde{\chi}(\omega)=\frac{2}{\pi}\int_0^\infty \tilde{\chi}''(\omega')\,d\omega'\int_0^\infty e^{i\omega t}\sin\omega' t\,dt\ . \tag{B5}$$

Carrying out the inner integral in Eq. (B5) and using $\tilde{\chi}''(-\omega)=-\tilde{\chi}''(\omega)$ gives

$$\tilde{\chi}(\omega)=\frac{1}{\pi}\int_{-\infty}^\infty d\omega'\,\frac{\tilde{\chi}''(\omega')}{\omega'-\omega}\ . \tag{B6}$$

Finally taking $\omega\to\omega+i\epsilon$, ω real, and $\epsilon\to 0$, and using the standard identity

$$\frac{1}{\omega'-\omega-i\epsilon}=P\left[\frac{1}{\omega'-\omega}\right]+i\pi\,\delta(\omega'-\omega)$$

gives Eq. (B1).

A parallel demonstration holds for $\Theta(t)$, since the Kramers–Kronig result is true for any causal response function.

APPENDIX C

We here develop a least action formulation of the generalized Langevin equation. This is important for the transition from classical to quantum mechanics.[5] Our result is that the scattering GLE equation (6.1) can be derived from the *two-particle* effective action functional

$$\mathcal{S}[x(t),\ Y(t)]=\int_0^T dt\left\{\tfrac{1}{2}M\dot{Y}^2(t)+\tfrac{1}{2}\dot{x}^2(t)-\tfrac{1}{2}\omega_0^2x^2(t)\right.$$
$$\left.-W[x(t),\ Y(t)]+\int_0^t ds\,x(t)\,\frac{\Theta(t)\Theta(T-s)}{\Theta(T)}\,x(s)+x(t)R(t)\right\}, \tag{C1}$$

via a least action principle

$$\delta\mathcal{S}[x(t),\ Y(t)]=0\ , \tag{C2}$$

where δ denotes variation of the trajectories $x(t)$ and $Y(t)$. Notice that Eqs. (C1) and (C2) differ from the conventional Lagrangian formulation of (nondissipative) classical mechanics[30] because of the many-body terms involving $R(t)$ and $\Theta(t)$ in $\mathcal{S}$.

We begin with the *full* gas/solid action $S[x(t),\ Y(t),\ \mathbf{x}_Q(t)]$, where $\mathbf{x}_Q(t)$ denotes the trajectories of the heat bath atoms.[31] We split it into a two-body and a many-body part; i.e., we write

$$S[x(t),\ Y(t),\ \mathbf{x}_Q(t)]$$
$$=S_1[x(t),\ Y(t)]+S_2[x(t),\ \mathbf{x}_Q(t)]\ , \tag{C3}$$

where the two-body contribution

$$S_1[x(t),\ Y(t)]=\int_0^T dt\,\{\tfrac{1}{2}M\dot{Y}^2(t)+\tfrac{1}{2}\dot{x}^2(t)$$
$$-\tfrac{1}{2}\omega_0^2x^2(t)-W[x(t),\ Y(t)]\}\ , \tag{C4}$$

and where

$$S_2[x(t),\ \mathbf{x}_Q(t)]=\int_0^T dt\,\{\tfrac{1}{2}\dot{\mathbf{x}}_Q^\dagger(t)\dot{\mathbf{x}}_Q(t)$$
$$-\tfrac{1}{2}\mathbf{x}_Q^\dagger(t)\,\omega_{QQ}^2\,\mathbf{x}_Q(t)-\mathbf{x}_Q^\dagger(t)\,\omega_{QP}^2\,x(t)\}\,dt \tag{C5}$$

is the action for the heat bath if driven by a force $-\omega_{QP}^2x(t)$.

The trajectories $Y(t)$, $x(t)$, $\mathbf{x}_Q(t)$ are arbitrary. It is the additional assumption of least action which leads to the classical trajectories. We now assume classical trajectories for the heat bath atoms; i.e., we assume[31]

$$\ddot{\mathbf{x}}_Q(t)=-\omega_{QQ}^2\,\mathbf{x}_Q(t)-\omega_{QP}^2\,x(t)\ , \tag{C6}$$

where $x(t)$ is arbitrary. Integrating the first term in Eq. (C5) by parts and using Eq. (C6) yields

$$S_2[x(t),\ \mathbf{x}_Q(t)]=\tfrac{1}{2}\mathbf{x}_Q^\dagger(t)\,\dot{\mathbf{x}}_Q(t)\,\Big|_0^T$$
$$-\frac{1}{2}\int_0^T dt\,\mathbf{x}_Q^\dagger(t)\,\omega_{QP}^2\,x(t)\ , \tag{C7}$$

where now $\mathbf{x}_Q(t)$ is that *classical* trajectory of the heat bath which satisfies the double ended boundary conditions $\mathbf{x}_Q(0)=\mathbf{x}_Q$ and $\mathbf{x}_Q(T)=\mathbf{x}_Q'$.

Equation (C6) can be solved to give $\mathbf{x}_Q(t)$ as a functional of $x(t)$. Substitution of the result in Eq. (C7) gives after much rearrangement

$$S_2[x(t),\ \mathbf{x}_Q(t)]=H[\mathbf{x}_Q',\ \mathbf{x}_Q;\ T]+\hat{S}[x(t)]\ , \tag{C8}$$

where

$$H[\mathbf{x}_Q',\ \mathbf{x}_Q;\ T]=\tfrac{1}{2}\mathbf{x}_Q'^\dagger\,\theta^{-1}(T)\,\dot{\theta}(T)\,\mathbf{x}_Q'$$
$$+\tfrac{1}{2}\mathbf{x}_Q^\dagger\,\theta^{-1}(T)\,\dot{\theta}(T)\,\mathbf{x}_Q-\mathbf{x}_Q^\dagger\,\theta^{-1}(T)\mathbf{x}_Q'\ , \tag{C9}$$

with $\theta(t)$ as defined elsewhere,[4] and where

$$\hat{S}[x(t)]=\int_0^T dt\left\{\int_0^t ds\,x(t)\,\frac{\Theta(t)\Theta(T-s)}{\Theta(T)}\,x(s)+x(t)R(t)\right\}. \tag{C10}$$

The random force[4]

$$R(t)=\omega_{PQ}^2\,[\,\dot{\theta}(t)\,\mathbf{x}_Q(0)+\theta(t)\,\dot{\mathbf{x}}_Q(0)] \tag{C11}$$

is expressed in terms of $\mathbf{x}_Q$ and $\mathbf{x}_Q'$ as

$$R(t)=\omega_{PQ}^2\left\{\theta^{-1}(T)[\,\theta(T-t)\,\mathbf{x}_Q+\theta(t)\,\mathbf{x}_Q']\right.$$
$$\left.+\int_0^T \Theta(t)\Theta^{-1}(T)\Theta(T-s)\,\omega_{QP}^2\,x(s)\,ds\right\}. \tag{C12}$$

$H(\mathbf{x}_Q',\ \mathbf{x}_Q;\ T)$ is independent of $x(t)$ and hence can be ignored when formulating a least action principle for $x(t)$ and $Y(t)$. Thus Eq. (C1) is derived by adding Eqs. (C4) and (C10). The scattering GLE is derived from Eq. (C1) by varying $x(t)$ and $Y(t)$ with $\mathbf{x}_Q$, $\mathbf{x}_Q'$, and T fixed using Eq. (C12).

*Alfred P. Sloan Foundation Fellow.

[1]For recent reviews of experimental and theoretical progress in gas/solid dynamics see for example J. N. Smith, Surf. Sci. 34, 613 (1973); J. P. Toennies, Appl. Phys. 3, 91 (1974); W. H. Weinberg, Adv. Colloid Interface Sci. 4, 301 (1975); and F. O. Goodman, Prog. Surf. Sci. 5, 261 (1974).
[2]S. A. Adelman and J. D. Doll, J. Chem. 61, 4242 (1974); 62, 2518 (1975).
[3]J. D. Doll, L. E. Myers, and S. A. Adelman, J. Chem. Phys. 63, 4908 (1975).

[4]S. A. Adelman and J. D. Doll, J. Chem. Phys. 64, 2375 (1976). For simplicity of notation we will specialize the results of this paper to a single struck atom and drop vector notation. Note Eqs. (1.1) give the GLE for the free lattice. The GLE for scattering is given by Eqs. (6.1).

[5]S. A. Adelman, Chem. Phys. Lett. 40, 495 (1976).

[6]$\Theta(t)$ is the response of the heat bath to an input $\delta(t)$; $\beta(t)$ is its response to $\zeta(-t)$ for $t>0$ where $\zeta(t)$ is the unit step function.

[7]See Sec. III.

[8]A generalization to anharmonic solids is given in S. A. Adelman, "Generalized Langevin Theory for Gas/Solid Processes: Linear Response Approximation for Anharmonic Solids," in preparation.

[9]B. J. Garrison and S. A. Adelman (unpublished results).

[10]R. P. Feynman and A. R. Hibbs, *Quantum Mechanics and Path Integrals* (McGraw-Hill, New York, 1965).

[11]The Laplace transform of an arbitrary function $f(t)$ is here denoted by $\hat{f}(z)$; i.e., $\hat{f}(z) \equiv \int_0^\infty e^{-zt} f(t)\, dt$.

[12]See for example A. A. Maradudin, E. W. Montroll, G. H. Weiss, and I. P. Ipatova, *Theory of Lattice Dynamics in the Harmonic Approximation* (Academic, New York, 1971), 2nd ed.

[13]The problem of calculating $\rho(\omega)$ has been considered by many authors since the work of E. Montroll, J. Chem. Phys. 10, 218 (1942); 11, 481 (1943). For a review of the earlier work see Ref. 12. More recent treatments have been given by J. Deltour, Physica 39, 413 (1968); R. I. Cukier and J. C. Wheeler, J. Chem. Phys. 60, 4639 (1974); O. Platz and R. G. Gordon, Phys. Rev. Lett. 20, 264 (1973).

[14]For a monatomic isotropic lattice one may always find a nearest-neighbor chain with identical mode density. One simply tridiagonalizes the force constant matrix for the original solid. The resulting tridiagonal form may be regarded as the force constant matrix for the equivalent chain. For anisotropic lattices the solid can be replaced by three chains.

[15]For example our trajectory studies showed that atoms trapped on 0 °K lattices modeled by a few undamped oscillators eventually desorbed!

[16]Another method for sampling noise is given by J. D. Doll and D. R. Dion, Chem. Phys. Lett. 37, 396 (1976).

[17]H. Mori, Prog. Theoret. Phys. 33, 423 (1965); R. Kubo, Rept. Prog. Theoret. Phys. 29, 255 (1966).

[18]R. Kubo, J. Phys. Soc. Jpn 12, 570 (1957).

[19]For a recent molecular dynamics simulation of a solid see B. Quentrec, Phys. Rev. B 12, 282 (1975).

[20]D. P. Jackson, Radiat. Eff. 18, 185 (1973).

[21]See for example, L. Padulo and M. A. Arib, *Systems Theory* (W. B. Saunders, Washington, 1974).

[22]M. W. Wang and G. E. Uhlenbeck, Rev. Mod. Phys. 17, 323 (1945); S. Chandrasekhar, *ibid* 15, 1 (1943).

[23]R. M. Logan and J. C. Keck, J. Chem. Phys. 49, 860 (1968).

[24]For theoretical calculations of the rainbow effect, see for example J. D. McClure, J. Chem. Phys. 51, 1687 (1969); 57, 2810 (1972); 57, 2823 (1972), and W. A. Steele, Surf. Sci. 38, 1 (1973). For experimental observations of the rainbow effect, see for example J. N. Smith, D. R. O'Keefe, and R. L. Palmer, J. Chem. Phys. 52, 315 (1970); 52, 4572 (1971); R. E. White, J. J. Ehrhardt, and R. P. Merrill, *ibid*. 64, 41 (1976).

[25]For theoretical calculations of diffraction see for example, G. Wolken Jr., J. Chem. Phys. 58, 3047 (1973); 61, 456 (1974); F. O. Goodman, Surf. Sci. 19, 93 (1970); J. D. Doll, Chem. Phys. 3, 257 (1974); J. Chem. Phys. 61, 954 (1974); R. I. Masel, R. P. Merrill, and W. H. Miller, J. Chem. Phys. 64, 45 (1976). For experimental studies see for example B. R. Williams, J. Chem. Phys. 55, 1315, 3220 (1971); W. H. Weinberg and R. R. Merrill, *ibid*. 56, 2893 (1972); A. G. Stoll Jr., J. J. Erhardt, and R. P. Merrill, *ibid*. 64, 34 (1976).

[26]We employed a fourth order Adams–Moulton predictor corrector integrator.

[27]This idea has often been exploited before. See for example M. Karplus, R. Porter, and R. D. Sharma, J. Chem. Phys. 43, 3259 (1965).

[28]R. Sau and R. P. Merrill, Surf. Sci. 34, 268 (1973).

[29]Y. W. Lin and G. Wolken, Jr., J. Chem. Phys. 65, 2634 (1976).

[30]H. Goldstein, *Classical Mechanics*, (Addison-Wesley, Reading, MA, 1965).

[31]We use the notation of Ref. 4.